Science of the Total Environment 586 (2017) 817–826

Contents lists available at ScienceDirect

Science of the Total Environment

journal homepage: www.elsevier.com/locate/scitotenv

Effects of monovalent and divalent metal cations on the aggregation and suspension of Fe_3O_4 magnetic nanoparticles in aqueous solution

Hao Wang [a,b], Xiaoli Zhao [b,*], Xuejiao Han [b], Zhi Tang [b], Shasha Liu [a,b], Wenjing Guo [a,b], Chaobing Deng [c], Qingwei Guo [d], Huanhua Wang [b], Fengchang Wu [b], Xiaoguang Meng [b,e], John P. Giesy [b,f]

[a] College of Water Sciences, Beijing Normal University, Beijing 100875, China
[b] State Key Laboratory of Environmental Criteria and Risk Assessment, Chinese Research Academy of Environmental Sciences, Beijing 100012, China
[c] Environmental Monitoring Center of Guangxi Zhuang Autonomous Region, Guangxi 530028, China
[d] South China Institute of Environmental Science, MEP, Guangzhou 510655, China
[e] Center for Environmental Systems, Stevens Institute of Technology, Hoboken, NJ 07030, United States.
[f] Department of Biomedical and Veterinary Biosciences and Toxicology Centre, University of Saskatchewan, Saskatoon, Saskatchewan, Canada

HIGHLIGHTS

- The hydration force and ionic radius of metal cations significantly affected the aggregation of MNPs.
- Metal cations affected the stabilities of MNPs in a decreasing order of $Ba^{2+} > Sr^{2+} > Ca^{2+} > Mg^{2+} > Na^{+}$.
- Divalent cations of low concentrations potentially enhanced the suspension of MNPs at acidic conditions.
- Divalent cations served as bridges to stabilize the aggregation of MNPs.

GRAPHICAL ABSTRACT

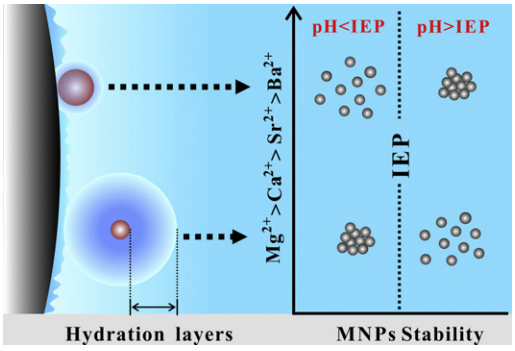

ARTICLE INFO

Article history:
Received 21 December 2016
Received in revised form 4 February 2017
Accepted 7 February 2017
Available online 12 February 2017

Editor: Jay Gan

Keywords:
Fe_3O_4 MNPs
Specific ion effects
Aquatic environment
Aggregation and suspension
Metal cations

ABSTRACT

There has been limited research investigating how the mechanisms of aggregation of magnetic nanoparticles (MNPs) are affected by inorganic ions. In this study, Na^{+}, Mg^{2+}, Ca^{2+}, Sr^{2+} and Ba^{2+} were selected to systematically study the aggregation mechanisms of Fe_3O_4 MNPs. The results indicated that divalent cations more significantly affected the stabilities of MNPs than Na^{+} at low concentrations (e.g., 0.1 mM) in a decreasing order of $Ba^{2+} > Sr^{2+} > Ca^{2+} > Mg^{2+} > Na^{+}$. Extended DLVO theory did not offer a satisfactory explanation for the above difference due because it ignores specific ion effects. It was also found that the initial adsorption ratios of these metals by Fe_3O_4 MNPs were linearly proportional to the hydrodynamic diameter (HDD) of Fe_3O_4 MNPs before aggregation occurred. In addition to the valence states, the hydration forces and ionic radii of the metal cations were proposed to be other factors that significantly affected the interactions of metal cations with Fe_3O_4 MNPs based on the excellent linear relationships of the HDD of Fe_3O_4 MNPs and these three factors. Moreover, a bridging function of divalent cations might develop after aggregation occurred based on the increases in their adsorption amounts and intensities for binding oxygen-containing functional groups. In addition, an increase in the positive ζ potential of MNPs was observed with the addition of divalent cations until 10.0 mM at a pH of 5.0, which potentially enhances the resistance of MNPs to aggregation in aquatic systems compared with Na^{+}. Consequentially, the effects of metal cations on the aggregation of MNPs are determined by the

* Corresponding author.
E-mail address: zhaoxiaoli_zxl@126.com (X. Zhao).

http://dx.doi.org/10.1016/j.scitotenv.2017.02.060

hydration forces, valance states, ionic radii and bond types formed on the MNPs. Thus, the specific ion effects of these cations should be considered in predicting the environmental behaviors of specific nanomaterials.

1. Introduction

Nanomaterials (NMs) have been applied in numerous fields for their small particle size, exceptionally large surface area, relatively great surface energy or other special properties compared with those of bulk materials (Klaine et al., 2008; Sun et al., 2016). Until now, registered nanoproducts have exceeded 1800 species, and they potentially impact the quality of the environment after inevitably being discharged into the environment during their production and use (Auffan et al., 2009; Fiorino, 2010; Klaine et al., 2008; Vance et al., 2015; Wang et al., 2015). Nanomaterials could accumulate in tissues of humans and wildlife and impair organelles, tissues, organs, and even cause tumors after being ingested by respiration, diet and so on (Borm et al., 2006; Fiorino, 2010; Wiesner et al., 2006). Due to their unique physical and chemical properties, magnetic nanoparticles (MNPs) have been extensively applied in several fields, but their dispersion in aquatic systems might result in adverse effects on aquatic organisms (Lu et al., 2007; Pankhurst et al., 2003; Reddy et al., 2012; Zhang and Elliott, 2006). Effects of NMs are a function of their forms in the environment, and free individual NMs behave differently than if they are aggregated (Albanese and Chan, 2011; Yu et al., 2016). In fact, aggregation generally reduces the availability of NMs and thus reduces their toxic potential and ability to cause adverse effects in aquatic animals or to be accumulated in food chains (Sharma, 2009). The suspension and aggregation of MNPs are more sensitive to the fluctuation of environmental conditions due to their super-paramagnetism and neutral IEP values compared with other nanoparticles (Zhao et al., 2008a; Zhao et al., 2008b). However, until now, how the underlying mechanisms of the aggregation of MNPs are affected by inorganic ions remains unknown, especially their special salt effects (Li et al., 2014; Philippe and Schaumann, 2014).

Water is a significant route for NMs to enter the environment (Farré et al., 2009; Moore, 2006; Wiesner et al., 2006). The pH, natural organic matter and inorganic ions are the main factors that influence the environment behaviors of NMs (Aiken et al., 2011; O'Brien and Cummins, 2011; Wu and Xing, 2009). Several research groups have reported that dissolved organic matter (DOM) significantly affected the suspension and aggregation of NMs in water by adsorbing onto the surface to form a coating by physical and chemical reactions such as electrostatic forces, cation bridging, and rigid polymer bridging (Baalousha, 2009; Bian et al., 2011; Chen and Elimelech, 2007; Christian et al., 2008; Johnson et al., 2009; Lin et al., 2010; Philippe and Schaumann, 2014; Saleh et al., 2010). Meanwhile, it was also reported that the resistance of some nanoparticles, such as TiO_2, ZnO, and Fe_2O_3, to aggregation could be affected by the types and concentrations of compounds in the aqueous phase along with their compositions, isoelectric point (IEP), particle size, surface coating and possibly other attributes (Bian et al., 2011; Chen and Elimelech, 2006, 2007; Zou et al., 2016a). Among these factors, the ion type and concentration play key roles in affecting the interaction of DOM with NMs in aquatic environments. The valences and concentrations of metal cations, such as Na^+, Mg^{2+} and Ca^{2+} that have been used as modulators of ionic strength (IS) in many studies, have been reported to significantly affect the aggregation of NMs in aquatic environments. Due to the higher ionic strength supplied by divalent cations, more counter ions would diffuse around the nanoparticles and screen the surface charge of the particles more than monovalent cations. Thus, they would heavily shorten the Debye length of the particles. Therefore, due to the greater charge screening and compression effects of the electric double-layer, divalent cations destabilize nanoparticles more efficiently than monovalent cations at similar concentrations (Badawy et al., 2010; Bizmark and Ioannidis, 2015; Chen and Elimelech, 2007; Chen et al., 2006; Chowdhury et al., 2013; French et al., 2009; Li et al., 2014; Saleh et al., 2008, 2010; Zhang et al., 2009). Many studies reported obvious differences for Na^+, Mg^{2+}, and Ca^{2+} in changing the ζ potential and hydrodynamic radius (HDD) of NMs, such as silver, graphene oxide, and carbon nanotubes, but they did not further explain the differences fundamentally (Chang and Bouchard, 2013; Chen and Elimelech, 2006; Chowdhury et al., 2013). For example, it has been found that Ca^{2+} could bind with hydroxyl and carbonyl functional groups and result in an increase of the HDD of graphene oxide (GO) nanoparticles, but Mg^{2+} did not have the same effect despite both cations changing the electrophoretic mobility of GO particles at the same level (Chowdhury et al., 2013). It was confirmed that Mg^{2+} accelerated the aggregation of alginate-coated hematite just through electrostatic destabilization and never formed inter-particle bridges as Ca^{2+} did. It was also suggested that other mechanisms, besides electrostatic interaction, could be involved in the aggregation of bacteriophages by Ca^{2+} and Mg^{2+} (Chen et al., 2006; Pham et al., 2009). Therefore, to assess environmental behaviors of nanoparticles accurately, it is necessary to systematically investigate the mechanisms of interaction between various ions and nanoparticles.

In this study, the effects of Na^+, Mg^{2+}, Ca^{2+}, Sr^{2+} and Ba^{2+} on the suspension and aggregation of Fe_3O_4 MNPs in aquatic systems were systematically investigated. The ζ potential and HDD of Fe_3O_4 MNPs were determined as functions of the valence and concentration of the ion. Extended Derjaguin-Landau-Verwey-Overbeek (DLVO) theory and adsorption behaviors of metal cations were also used to further explore the interactions of MNPs with metal ions. The results of the study provided basic information to understand the behaviors of other NMs in aquatic environments.

2. Materials and methods

2.1. Materials

NaOH (96.0%) and HCl (36.0%–38.0%) were purchased from Beijing Chemical Works. $FeCl_2 \cdot 4H_2O$ (98.0%) and ammonia (NH_3) solution (25–28%) were purchased from the Xilong Chemical Industry Incorporated Co. Ltd. (Guangdong, China). $FeCl_3 \cdot 6H_2O$ (99.0%), NaCl (99.8%), $MgCl_2 \cdot 6H_2O$ (98.0%), $CaCl_2 \cdot 2H_2O$ (99.0%), $SrCl_2 \cdot 4H_2O$ (99.5%), and $BaCl_2 \cdot 4H_2O$ (99.5%) were purchased from the Sinopharm Chemical Reagent Co., Ltd. (Beijing, China). All of the experimental water (ultrapure water, 18.2 MΩ·cm) was supplied by a Millipore Integral 5 water purification system (Merck, Germany).

2.2. Experiment and theoretical analysis

Fe_3O_4 MNPs used in experiments were synthesized by co-precipitation (Zhao et al., 2008a). Detailed information on the preparation of the MNPs is given in the supporting information (SI). Meanwhile, for the particle aggregation study, 100.0 μL of the Fe_3O_4 MNP solution (20 $mg \cdot mL^{-1}$) was added separately to 40 mL of an oxygen-free solution of NaCl, $MgCl_2$, $CaCl_2$, $SrCl_2$ or $BaCl_2$, where the nominal concentrations of the metal cations were 0, 0.01, 0.1, 1.0, 10.0, 50.0 and 100.0 mM based on that the concentrations of these metal cations are generally <100.0 mM in a natural aquatic environment (Boyd and Thunjai, 2003; Guo et al., 2001; Jalali and Jalali, 2016). The pH of each sample was adjusted to 5.00 ± 0.04 with only HCl (0.1 M) or 9.00 ± 0.04 with only $NH_3 \cdot H_2O$ (1.0 M) with monitoring by the use of a pH probe (FE20K, Mettler Toledo, Switzerland) due to that the pH of natural water is generally in the range of 5.0–9.0 (Chowdhury et al., 2013;

Crittenden et al., 2012; Hem, 1970). The HDD and ζ potential values of Fe_3O_4 MNPs were analyzed via dynamic light scattering (DLS) and laser Doppler velocimetry (LDV) techniques, respectively, and both were measured with a Zetasizer Nano (Malvern, England) (Baalousha and Lead, 2012). Vials were washed with ultrapure water several times after standing in HCl solution overnight, and then, they were dried at 150 °C for >4 h before use. Three replicates of each sample were analyzed. The concentrations of metal cations before and after adsorption were analyzed with an inductively coupled plasma optical emission spectrometer (ICP-OES, Optima 5300 DV, PerkinElmer, Massachusetts, USA). The magnetic properties of the MNPs were characterized with a vibrating sample magnetometer (VSM, LDJ9600 USA). High-resolution transmission electron microscopy (HRTEM, JEM-2100F, JEOL, Japan) was employed to characterize the Fe_3O_4 MNPs used in the study, and the control voltage was 200 kV. The surface elemental composition of samples was analyzed with X-ray photoelectron spectroscopy (XPS, PHI Quantera SXM, ULVAC-PHI, Japan) with a monochromated X-ray beam (100 μm) from an Al target at an angle of 45°, and the binding energy was calibrated with C1s of 284.8 eV.

Theoretical analysis of the aggregation of MNPs is described in the SI.

3. Results and discussion

3.1. Effect of the pH on the ζ potential and HDD of MNPs

The MNPs of the study had a size of approximately 10 nm, and could be assumed to be single magnetic domain particles based on the characteristics of MNPs (Fig. S1 in the SI). The ζ potential of MNPs decreased from 30 mV to −40 mV as the pH of the solution increased from 5.0 to 12.0 (Fig. 1a). When the pH of the solution was in the range of 6.0–8.0, the ζ potential of MNPs was <20 mV, and the HDD of MNPs also increased from 250 nm to >2000 nm (Fig. 1b), which suggested that aggregation of MNPs could occur with decreased electrostatic repulsion between MNPs due to the weakening of the ζ potential (Godinez and Darnault, 2011). At a pH of approximately 5.0, the Fe-OH functional groups on the surface of MNPs could be protonated to generate Fe-OH_2^+, and as a result, the dispersion of MNPs could be stabilized and the aggregation minimized. As the pH of the solution increased to 9.0, the Fe-OH could deprotonate to form Fe-O^-, which gradually changed the sign of the surface charge of the MNPs and increased the negative charge of the MNPs, thus resulting in a decrease of the HDD of the MNPs (Illés and Tombácz, 2006). Thus, the diffusion of MNPs would be greater under more alkaline or acidic conditions, which would tend to minimize the aggregation of MNPs (Berg et al., 2009). In addition, the type and number of functional groups on the surface of MNPs depend on the pH of the sample, and the IEP of MNPs was observed to be approximately 7.1 from Fig. 1a, which means the physicochemical properties of MNPs at a pH below 7.1 are very different from those at a pH above 7.1 in an aquatic environment. Therefore, the effects of metal cations on the stability of MNPs should be separately analyzed in acidic and alkaline conditions. Actually, in the aquatic phase, hydration layers are formed around the surfaces of MNPs and ions (e.g., Na^+, Mg^{2+} and Ca^{2+}) by hydrogen bonds due to the interaction between the surface functional groups and water molecules (Bagchi, 2005; Grasso et al., 2002; Zou et al., 2016b). The hydration layers could also affect the interactions between MNPs and ions, and thus should be considered in studying the effects of metal cations on the aggregation of MNPs.

3.2. Effects of metal cations on the suspension and aggregation of MNPs at a pH of 5.0

At a pH of 5.0, more Fe-OH_2^+ functional groups were formed on the surface of MNPs, and the sign of charge on particle surface is therefore positive, with the ζ potential for MNPs being approximately 30 mV (Illés and Tombácz, 2006). The effect of Na^+, Mg^{2+}, Ca^{2+}, Sr^{2+} or Ba^{2+} on the ζ potential for MNPs could be divided into two stages. During the first stage, at concentrations <10.0 mM, as the concentration of each divalent cation increased, the ζ potential of MNPs increased significantly (Fig. 2a). In contrast, Na^+ had little effect on the ζ potential of MNPs at the same concentration. According to Coulomb's law, the electrostatic attraction of Fe-O^- to each divalent cation is much stronger than that for monovalent cations, and as a result, a divalent cation could be more competitively adsorbed on the surface of MNPs with a hydrogen atom. Thus, the adsorbed Mg^{2+}, Ca^{2+}, Sr^{2+} or Ba^{2+} could clearly increase the ζ potential of MNPs. Due to the same valence states of Na^+ and H^+, the adsorbed Na^+ could not significantly change the ζ potential of MNPs. However, divalent cations increased the ζ potential of MNPs differently with a trend of $Ba^{2+} > Sr^{2+} > Ca^{2+} > Mg^{2+}$, which indicated that some other factors could also change the ζ potential of MNPs, such as the hydration ability of the ions. In the aquatic phase, metal cations can interact with water molecules to form a hydration shell around themselves, and the intensity of the interaction of different ions with water molecules depends on the physicochemical properties, such as the electronic structure, atomic weight and ionic radius. According to the sequence of ionic kosmotropes and chaotropes, the hydration ability of positive ions could be generally ordered as follows: $Na^+ < H^+ < Ba^{2+} < Sr^{2+} < Ca^{2+} < Mg^{2+}$ (Chaplin, 2008; Rodgers and Armentrout, 2016; Rodriguez-Cruz et al., 1999). A strongly hydrated cation could strengthen the hydrogen bonds around it and weaken other hydrogen bonds accepted by its surrounding water molecules, which may reduce the interaction of metal cations with the functional groups of MNPs (Ben Ishai et al., 2013; Chaplin, 2008). A weakly hydrated ion may be expelled from water molecules by strong water-

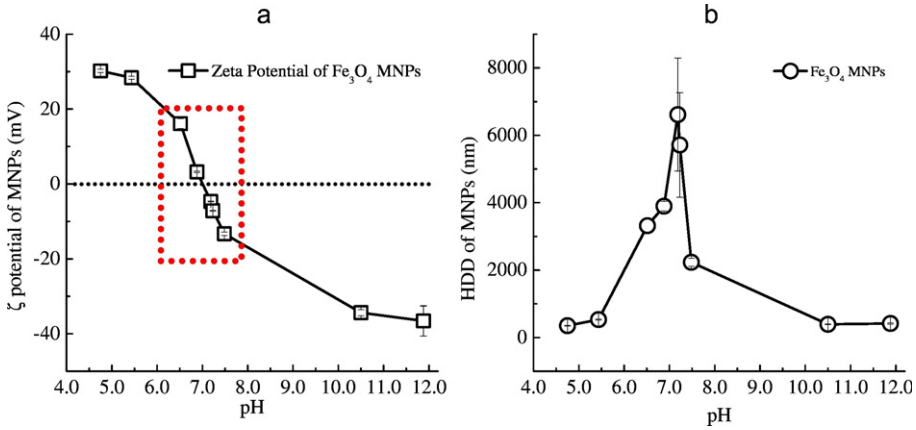

Fig. 1. Effects of pH on the ζ potentials (a) and hydrodynamic diameters (b) of Fe_3O_4 MNPs.

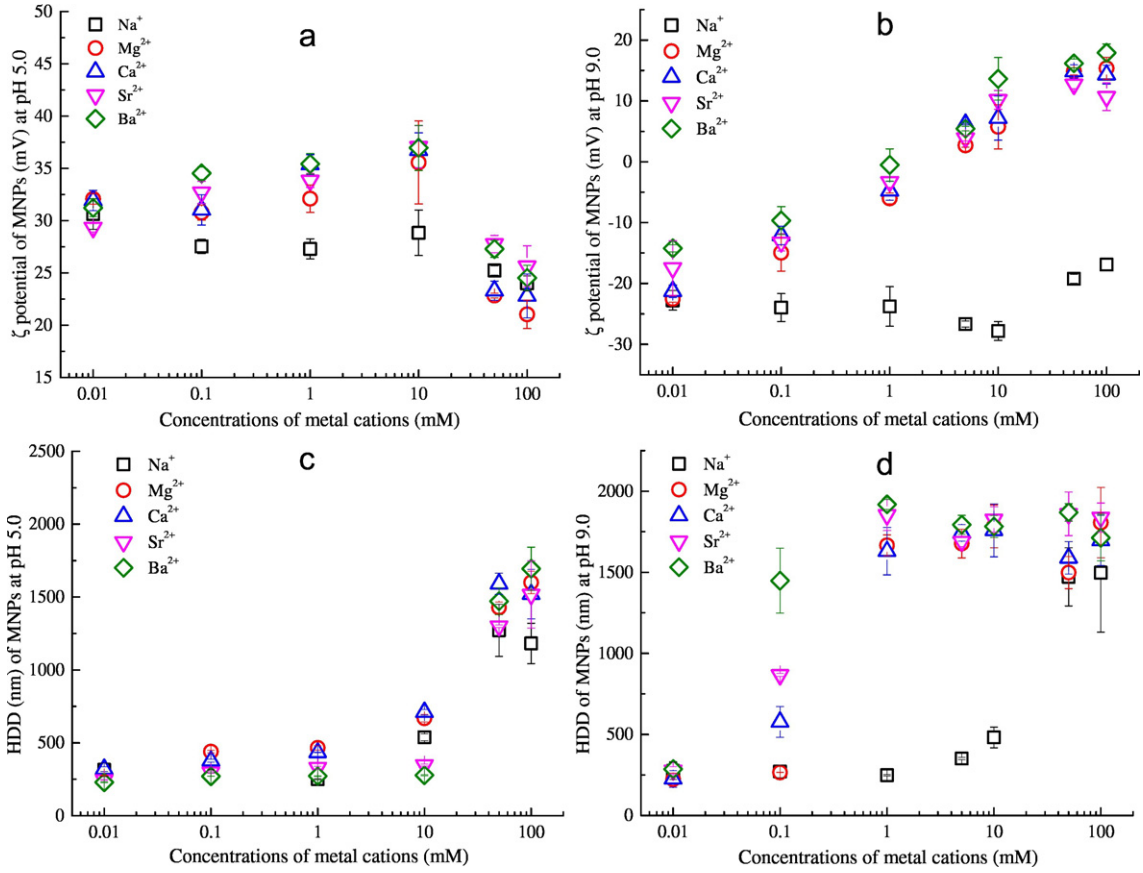

Fig. 2. Effects of the concentration of the five metal cations on the ζ potentials and HDD of Fe_3O_4 MNPs at a pH of 5.0 or 9.0. (a) ζ potential at a pH of 5.0, (b) ζ potential at a pH of 9.0, (c) HDD at a pH of 5.0, and (d) HDD at a pH of 9.0.

water interactions (hydrogen bonding), which may promote the adsorption of metal cations by MNPs (Ben Ishai et al., 2013; Chaplin, 2008). In this case, Na^+ might be pushed to the surface of MNPs by water molecules compared with divalent cations, and for the same reason, the different hydration capacities of divalent cations could also affect their adsorptions by MNPs. Therefore, the specific mechanism should be further explored based on the adsorption characteristics of the ions (section 3.5). As Fig. 2c shows, at concentrations below 10.0 mM, divalent cations gradually increased the ζ potential of MNPs, with the addition of these ions strengthening the inter-particle repulsion and stabilizing the suspension of MNPs. Additionally, the size of MNPs did not grow significantly as was the tendency for at a pH of 9.0.

During the second stage, ζ potentials of MNPs clearly declined when the concentrations of the cations were >10.0 mM (Fig. 2a), which might be due to the significant shrinkage of the EDLs of MNPs induced by the higher ion concentrations. For example, although the ζ potential of MNPs increased to >35 mV at 10.0 mM, the size of MNPs started increasing. However, the five metal cations presented different levels of influence on the size of MNPs due to their different properties. As the concentration of divalent cations increased to 100.0 mM, the size of MNPs increased to >1500 nm. Due to that the electrostatic repulsion between MNPs decreased with the continuous compression of EDLs, the distance between nanoparticles became much shorter under the effects of van der Waals and magnetic forces that developed from dipole-dipole attraction between different magnetic particles (Butter et al., 2003; Phenrat et al., 2007). In contrast, although Na^+ did not change the ζ potential of MNPs, for the same reason, its increased ionic strength also improved the size of the MNPs, especially at 10.0 mM and 100.0 mM (Fig. 2c). Additionally, given the different tendencies for the ζ potential of MNPs before and after the aggregation occurred, the binding forms and amounts of metal cations on the MNPs might also be different. Therefore, adsorption behaviors of these metal cations need to be systematically investigated.

3.3. Effects of metal cations on the suspension and aggregation of Fe_3O_4 MNPs at a pH of 9.0

At a pH of 9.0, due to the decreased competitive adsorption of hydrogen protons with the metal cations on the nanoparticle surface, all cations could be adsorbed much easier on the nanoparticle surface compared with in acidic conditions. According to the results in Fig. 2b and d, the effects of the cations could also be divided into two stages. During the first stage, divalent cations rapidly diminished the ζ potential of MNPs to 0 mV from roughly −25 mV as their concentrations increased to 1.0 mM from 0.01 mM (Fig. 2b). According to Coulomb's law, the main reason for this phenomenon could be the higher electrostatic attraction between divalent cations with electronegative functional groups compared with monovalent cations (e.g., Na^+ and NH_4^+) (Grasso et al., 2002). Meanwhile, due to the decrease of the electrostatic repulsion of inter-nanoparticles, the aggregation of MNPs occurred under the effect of van der Waals force, and as a result, the HDD of MNPs increased to >1500 nm from the initial 250 nm, even if the ζ potential of MNPs also increased to 15 mV at 10.0 mM once again (Fig. 2b and d). In contrast, the addition of Na^+ did not significantly change the ζ potential of MNPs, which might be attributed to the less electrostatic attraction between Na^+ and Fe-O^- as well as the effect of NH_4^+ that was used to adjust the pH. For monovalent ions, it was reported that NH_4^+ could make the electronegative colloidal suspension more unstable than Na^+ (López León et al., 2005).

During the second stage, the ζ potential of MNPs was not significantly changed and generally stayed at 15 mV with the addition of divalent cations from 10.0 mM to 100.0 mM (Fig. 2b). In contrast, the ζ potential

of MNPs increased from −27 mV to −16 mV with the introduction of Na^+ with a concentration >10.0 mM (Fig. 2d). This increase might be due to the greater ionic strength of the solution (Chen et al., 2006). In addition, at the same concentrations, the cations increased the ζ potential of MNPs in the following order: $Ba^{2+} > Sr^{2+} > Ca^{2+} > Mg^{2+} > Na^+$. This trend seems to be directly proportional (positively correlated) with their atomic masses and/or ionic diameters or possibly charge density. According to specific ion effects, the five cations listed above have different capacities for polarizing arrangements of their surrounding water molecules according to the following ranking: $Mg^{2+} > Ca^{2+} > Sr^{2+} > Ba^{2+} \approx Na^+$ (Förstner and Wittmann, 2012; Kunz, 2010). The relatively stronger hydration ability of the cations on the left of this order weakened their interaction with functional groups of MNPs. In contrast, the cations on the right of the order had to undergo more repulsion by the strong water-water interactions around themselves, which may promote their adsorptions onto the particles (Chaplin, 2008; López León et al., 2005; Lo Nostro and Ninham, 2012). Therefore, the affinity of the cations could be ranked as follows: $Na^+ \approx Ba^{2+} > Sr^{2+} > Ca^{2+} > Mg^{2+}$. However, due to the lower electrostatic attraction between Na^+ and nanoparticles, the ζ potential of MNPs hardly changed at the concentrations below 10.0 mM. Therefore, the capacity of the cations to promote aggregation of MNPs can be ranked as follows: $Ba^{2+} > Sr^{2+} > Ca^{2+} > Mg^{2+} > Na^+$.

Remarkably, there were significant differences between the cations in aggregating MNPs at 0.1 mM since relatively higher concentrations (≥0.1 mM) of these cations might result in a great decrease of the electrostatic repulsion of MNPs as well as significant compression of the EDLs and then lead to the aggregation of MNPs (Fig. 2d). Therefore, 0.1 mM could be the optimal concentration for further studying the reaction mechanism between MNPs and each metal cation. In addition, without the interference of the hydrogen protons in alkaline conditions, the five metal cations presented different and regular behaviors in the aggregation of MNPs compared with those at a pH of 5.0; hence, their reaction mechanisms could be analyzed in alkaline conditions. Moreover, when the concentration of Na^+ was 50.0 mM or 100.0 mM, the ζ potential of MNPs was approximately −20 mV, and it did not reverse to positive values as for divalent cations. This indicated that there likely was a different mechanism for the interaction of monovalent and divalent metal ions with MNPs, such as a bridging effect. For example, it has been reported that Ca^{2+} can serve as a bridge between molecules of DOM on the surface of nanoparticles, which results in the flocculation of MNPs. However, Mg^{2+} was unable to serve as a bridge (Chowdhury et al., 2013; Johnson et al., 2009). Such effects of cations on bare nanoparticles will be further discussed in section 3.5.

3.4. Theoretical analysis of the aggregation of MNPs

In traditional DLVO theory, electrostatic repulsion (V_{ESR}) and V_{vdW} mainly dominate the aggregation of colloids in aqueous environments. However, magnetite with a size below 80 nm could be regarded as single domain particle, and the inherent magnetic dipole moment in MNPs also affects their suspension or aggregation in the aquatic phase (Butler and Banerjee, 1975; Phenrat et al., 2007). It was commonly observed that the dipoles of iron particles could be arranged in a head-tail configuration even without an applied magnetic field (Butter et al., 2003; de Vicente et al., 2000). This behavior might also affect the stability of MNPs in an aquatic environment. The Hamaker constant is a key parameter in calculating the V_{vdW} between MNPs (Eq. (S2) in the SI). This is related to the temperature of the matrix and chemical composition of the MNPs. The Hamaker constant of MNPs generally ranges from 2.0×10^{-20} to 4.0×10^{-20} J, and the recommended value of 3.3×10^{-20} J is adopted in this study (Amal et al., 1990; Faure et al., 2011; Scholten, 1983).

Based on extended DLVO theory, a net energy barrier (NEB) was produced between MNPs at concentrations of metal cations <10.0 mM, and it was gone when the concentrations of these metal cations were at 100.0 mM (Fig. 3a). With the addition of the four divalent cations, the NEB of the MNPs strengthened first at 0.1 mM and then gradually decreased to zero at 100.0 mM. Based on Fig. 2a, the ζ potential of MNPs was clearly strengthened by divalent cations at concentrations below 10.0 mM, and as a result, the V_{EDL} was increased according to eq. S3. Therefore, the increase of the NEB might contribute to the much greater increased V_{EDL} compared with the attraction energies (V_{vdW} and V_M) between MNPs at 0.1 mM. The EDLs of MNPs were significantly shrunk under the relatively higher ion concentrations of samples. The NEB of MNPs significantly decreased under the combined effect of van der Waals force and magnetic attraction once the concentrations of divalent cations were beyond 0.1 mM. At a pH of 9.0, the NEB of MNPs significantly decreased to zero as the concentration of divalent cations increased to 1.0 mM (Fig. 3b). In contrast, Na^+ never changed the NEB of MNPs until its concentration reached 100.0 mM. The theoretical calculation was consistent with the results in Fig. 2. Therefore, the extended DLVO theory can work well to predict the dispersion or aggregation of MNPs in an aquatic environment for low salt concentrations.

However, the extended DLVO theory can hardly reveal the mechanism of interaction between metal cations and MNPs. For example, at a pH of 5.0, the monovalent cation Na^+ just decreased the NEB of MNPs, while the divalent cations could raise it from 0.01 mM to 0.1 mM. The capacity of the five cations for diminishing the NEB could be ranked as follows: $Na^+ > Mg^{2+} > Ca^{2+} > Sr^{2+} > Ba^{2+}$ (Fig. 3a and Fig. S2a). In contrast, at a pH of 9.0, the effects of these cations on diminishing the NEB could be ordered as follows: $Ba^{2+} > Sr^{2+} > Ca^{2+} > Mg^{2+} > Na^+$ (Fig. 3b and Fig. S2b). The sequence order of the five metal cations for electropositive MNPs (pH = 5.0) is the inverse of that observed for electronegative ones (pH = 9.0). The same phenomenon has been reported by several other groups, and specific ion effects were introduced to explain the interaction mechanisms (Bourikas et al., 2001; López León et al., 2003; Lo Nostro and Ninham, 2012). For example, it was reported that the sequence order of ions that affect the stability of protein, silica and TiO_2 in acidic conditions was generally opposite to that at alkaline conditions, and the sign of the interface charge is a key factor during the process (Dumont et al., 1990; Franks, 2002; López León et al., 2005). The above differences cannot be well explained by the current DLVO theory. Therefore, specific ion effects on the stability of the colloid or nanomaterial should be discussed in detail.

3.5. The adsorption of metal cations onto MNPs

According to the above discussion, the effects of five cations on the aggregation of MNPs were significantly different at concentrations below 10.0 mM. Specifically, at a pH of 5.0, under the effect of electrostatic attraction, the adsorption of metal ions by MNPs generally increased initially at concentrations below 0.5 mM (Fig. 4a). However, compared with Na^+ that reached its saturation adsorption of 1.44 ± 0.02 $mM \cdot g^{-1}$ at concentrations above 0.5 mM, absolute amounts of the four divalent cations adsorbed onto MNPs increased gradually with the addition of these cations and were nearly less than the half of the amount of adsorbed Na^+ at the same concentration points (<2.0 mM). Hence, at concentrations <2.0 mM, the amount of Na^+ adsorbed by MNPs was significantly larger than those of divalent cations (Fig. 4a). This observation could be consistent with the deduction in section 3.2 that metal cations with a lower hydration ability could be more easily adsorbed onto MNPs due to their relatively lower interactions with surrounding water molecules (Chaplin, 2008; Oncsik et al., 2015; Parsons et al., 2011). Additionally, according to Figs. 2a and 4a, both the amount of adsorbed divalent metal cations and ζ potential of MNPs always increased for concentrations from 0.01 to 5.0 mM at a pH of 5.0, indicating that the ion-exchange process on the surface of MNPs might be Fe-O···M^{2+} besides Fe-O···M^{2+}···O-Fe due to attraction of the hydrated water. Furthermore, with the addition of the metal cations, the adsorption ratios of them were generally ranked as

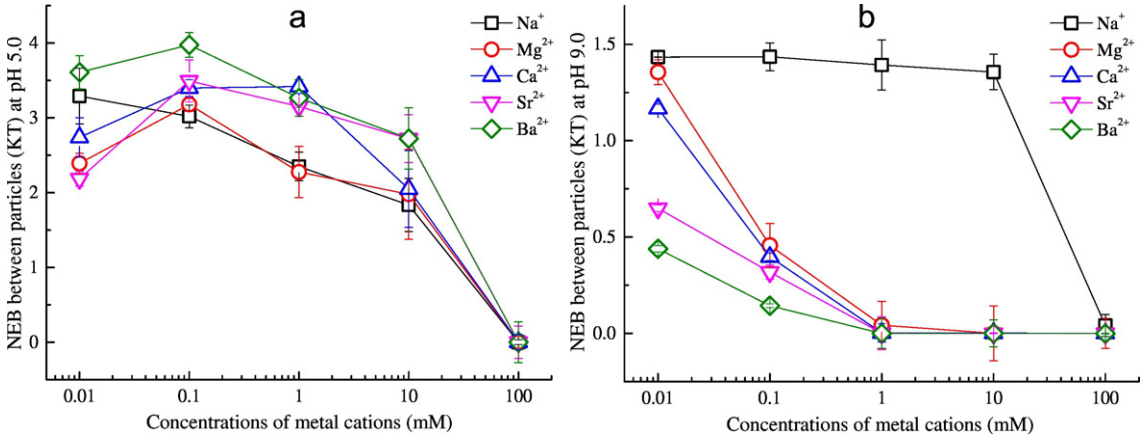

Fig. 3. Net energy between Fe_3O_4 MNPs as a function of the concentration of the five metal cations at a pH of 5.0 (a) or 9.0 (b).

$Na^+ > Ba^{2+} > Sr^{2+} > Ca^{2+} > Mg^{2+}$ at the concentration points from 0.01 to 0.1 mM (Fig. 4c). Such differences may also be regarded as a response to the effect of their different hydration forces during the adsorption process. Therefore, in this case, the electrostatic attraction between MNPs and metal cations cannot be responsible for the increase of the ζ potential in Fig. 2a based on Coulomb's law, and the dipole-dipole attraction between divalent metal cations and water molecules could be another significant factor for such behavior (Boström et al., 2001; Grasso et al., 2002). In addition, as the ion concentration increases, the aggregation of MNPs occurred, and the amounts of adsorbed divalent cations exceeded the maximum amount of adsorbed Na^+ on MNPs at 5.0 mM. This result indicated that divalent cations could be able to bind to more other adsorption sites of MNPs after the aggregation occurred. These sites might be located in the interstice of adjoining particles, and they could not be easily accessed by Na^+ due to its lower electrostatic attraction. However, there were no obvious differences in the amounts of the four divalent cations adsorbed on surfaces of MNPs, and the interference of hydrogen protons might contribute to the process.

The effects of hydrogen protons on the interactions between MNPs and 0.1 mM metal cations were evaluated at various pH values from 5.0 to 9.0. The results showed that differences in the effects of the five

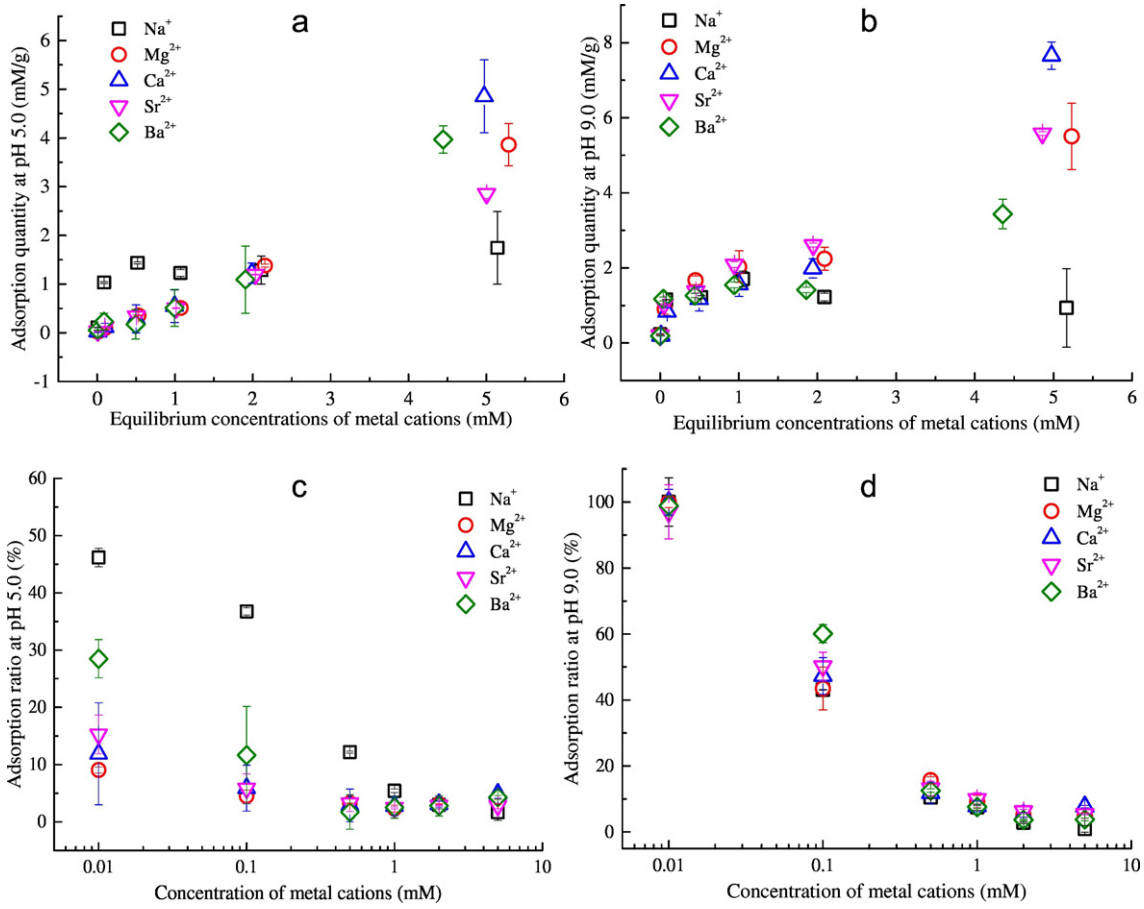

Fig. 4. Absolute adsorption amounts of the five metal cations by Fe_3O_4 MNPs as a function of their concentration at pH values of 5.0 (a) and 9.0 (b); adsorption ratios of the five metal cations by Fe_3O_4 MNPs as a function of their concentration at pH values of 5.0 (c) and 9.0 (d).

cations on the ζ potential of MNPs gradually emerged as the pH of the sample increased (Fig. S3). Therefore, hydrogen protons significantly affect the adsorption behaviors of metal cations on the surface of MNPs. The batch experiment conducted under alkaline conditions could be much better for studying the interaction mechanisms between metal cations and MNPs.

At a pH of 9.0, the absolute amounts of the five cations adsorbed by Fe_3O_4 MNPs all increased to 1.8 ± 0.2 mM·g^{-1} as a function of the concentration of the metals at concentrations >1.0 mM (Fig. 4b). Greater adsorption of metal ions occurred at a pH of 9.0 than that observed at a pH of 5.0. One possible reason for this result was the reduced competitive adsorption of hydrogen protons onto the active sites of MNPs at a pH of 9.0. As the addition of the metal cations increased from 0.01 mM to 1.0 mM, compared with Na^+ that formed only Fe-O···Na^+, divalent cations adsorbed onto the surface of MNPs might form Fe-O···M^{2+} or Fe-O···M^{2+}···O-Fe structures, which could neutralize the negative charges of the MNPs. Such a difference could well explain the significant increase in the ζ potential of MNPs in Fig. 2a and b. Additionally, there were no significant differences for the Na^+ adsorbed in the concentration range from 0.1 to 1.0 mM (Fig. 4b), which indicated that saturation adsorption of Na^+ by MNPs had been achieved and all of the exposed adsorption sites on the surfaces of MNPs were occupied by Na^+.

However, the adsorption ratios of the cations clearly decreased in the order Ba^{2+} (60%) > Sr^{2+} (50%) > Ca^{2+} (47%) > Mg^{2+} (47%) > Na^+ (43%) at 0.1 mM (Fig. 4d), which cannot be explained by electrostatic attraction or traditional DLVO theory. Thus, the adsorption of metal cations on MNPs could be controlled by other forces, especially for divalent cations. It was reported that more polarizable nanotubes presented stronger attractive interactions with gold nanoparticles (Rance et al., 2010). The metal cations in the study also presented different affinities for water molecules (Rodriguez-Cruz et al., 1999). Therefore, the polarizability of ions or nanomaterials largely affected their interaction with surrounding chemicals, and a hydration shell could be formed around the metal cations as well as on the surface of MNPs. The dipole-dipole attraction of cations with water near the surface of nanoparticles should be considered because metal cations concentrated in the region that is close to the particle surface are under the effect of electrostatic attraction. It has been reported that multi-hydrates were formed around alkaline or alkaline earth metals, and the binding energies of the above metal cations is in the order: $Mg^{2+} > Ca^{2+} > Sr^{2+} > Ba^{2+} > Na^+$, which might indirectly influence the capacities of MNPs to adsorb divalent cations (Rodgers and Armentrout, 2016; Rodriguez-Cruz et al., 1999).

Linear correlation between the HDD of Fe_3O_4 MNPs and the adsorption of the five metal cations was observed at 0.1 mM and a pH of 9.0 (Fig. 5a). This might indicate that adsorbed metal cations significantly affected the aggregation of Fe_3O_4 MNPs during the initial stages of aggregation. It has been reported that the hydration of metals could be one factor to determine the aggregation of NMs because a metal cation with a larger radius binds less tightly to water molecules than a smaller one (Pashley, 1981; Pashley and Israelachvili, 1984; Pham et al., 2009). Additionally, the hydration capacities of metal cations in group IA or IIA are significantly and positively correlated with the reciprocals of their ionic radii (Rodgers and Armentrout, 2016; Rodriguez-Cruz et al., 1999). The above reasons might indirectly promote the adsorption of larger metal cations by Fe_3O_4 MNPs. Furthermore, according to the Schulze–Hardy rule, the aggregation of NMs is influenced by the valences of metal cations (Sano et al., 2001; Verrall et al., 1999). According to the results of the study, significant linear correlation between the HDD of Fe_3O_4 MNPs was observed with the forces of hydration, valence states and ionic radii of the metal cations (Fig. 5b), and this correlation can be described as follows:

$$V_{HDD} \propto \frac{R^3 Z^6}{E}$$

where V_{HDD} is the HDD of Fe_3O_4 MNPs (nm); R is ionic radius; Z is the valence; and E is the hydration energy of the metal cation (kJ·mol^{-1}) (Table 1).

As the concentrations of metal cations exceeded 1.0 mM, the amounts of adsorbed divalent cations increased more significantly, but the amount of Na^+ decreased slightly (Fig. 4a and b). Moreover, the HDD of MNPs reached its maximum (approximately 1700 nm) at 5.0 mM for divalent cations; however, MNPs just started to aggregate at 5.0 mM for Na^+ (Fig. 2d). This might also indicate that divalent cations were able to be adsorbed in the interstice of MNPs and might form Fe-O···M···O-Fe between different particles (Seiichi et al., 2006). The adsorbed Na^+ might be expulsed from aggregated MNPs.

The adsorption of Na^+, Mg^{2+}, Ca^{2+}, Sr^{2+} and Ba^{2+} on MNPs was observed by using XPS technology (Fig. 6f). The binding intensities of metal cations with Fe-O- were quantified with the Lorentzian-Gaussian distribution (Fig. 6a, b, c, d and e). Given the interference of water and CO_2 molecules in the determination of MNPs with XPS, the photopeak of O 1s in Fig. 6 was de-convoluted into three other peaks containing 532.3 eV for O-H, 531.4 eV for C-O, and 530.0 eV for Fe-O, besides peaks for the adsorbed metal cations (Coppa et al., 2003; Yamashita and Hayes, 2008). The photopeaks of Fe-O-Na, Fe-O-Mg, Fe-O-Ca, Fe-O-Sr, Fe-O-Ba were fixed at 530.5, 530.9, 531.4, 530.5, and 529.5 eV, respectively (Ardizzone et al., 1997; Dumbre et al., 2014; Ghijsen et al., 1981; McGrail et al., 2001; Vasquez, 1991). The results presented that the binding areas for Na^+, Mg^{2+}, Ca^{2+}, Sr^{2+} and Ba^{2+} were 1882.0, 3245.9, 3644.0, 4120.4 and 5438.5 eV, respectively (Fig. 6). These results indicated that the intensities of divalent cations were nearly two times

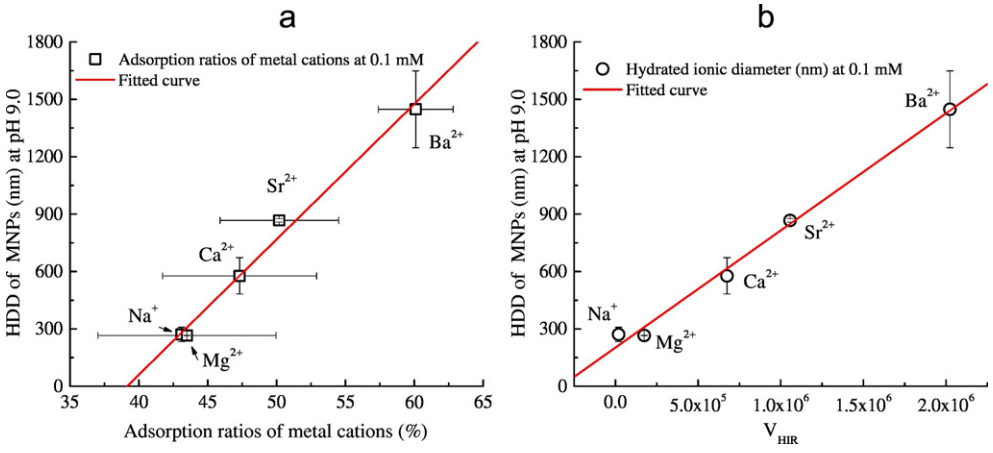

Fig. 5. Linear correlations of the HDD of Fe_3O_4 MNPs with the (a) adsorption ratios and (b) V_{HDD}.

Table 1
Parameters of metal cations.

Metal cations	Relative atomic mass[a]	Ionic radius (pm)[a]	Hydration energy ($kJ \cdot mol^{-1}$)[b]	Valence	Adsorption rate (%) at 0.1 mM[c]
Na	23.0	95	45.0	1	43.1 (0.1)
Mg	24.3	65	101.3	2	43.5 (6.5)
Ca	40.1	99	92.1	2	47.3 (5.6)
Sr	87.6	113	87.5	2	50.2 (4.3)
Ba	137.3	135	77.8	2	60.1 (2.7)

[a] The values were incited from the literature (House and House, 2015).
[b] The values were incited from the literature (Dzidic and Kebarle, 1970; Rodriguez-Cruz et al., 1999).
[c] The values were from this study.

that of Na^+, and they increased with their relative atomic weight. According to Figs. 2d and 4b, at a 5.0 mM concentration, the MNPs aggregated and the size stayed at approximately 1700 nm under the effect of divalent cations, and the amounts of adsorbed divalent cations increased sharply. In contrast, the MNPs just started to aggregate under the effect of Na^+, and the amount of adsorbed Na^+ declined slightly, which indicated that Na^+ might be expelled from the aggregates. In summary, divalent cations could not be expelled from the aggregated MNPs, and instead, they were also able to obtain more adsorption sites. Moreover, their binding intensities for oxygen-containing functional groups were much stronger than that of Na^+. Therefore, these results indicated that a bridging effect of divalent cations might occur between MNPs after aggregation occurred.

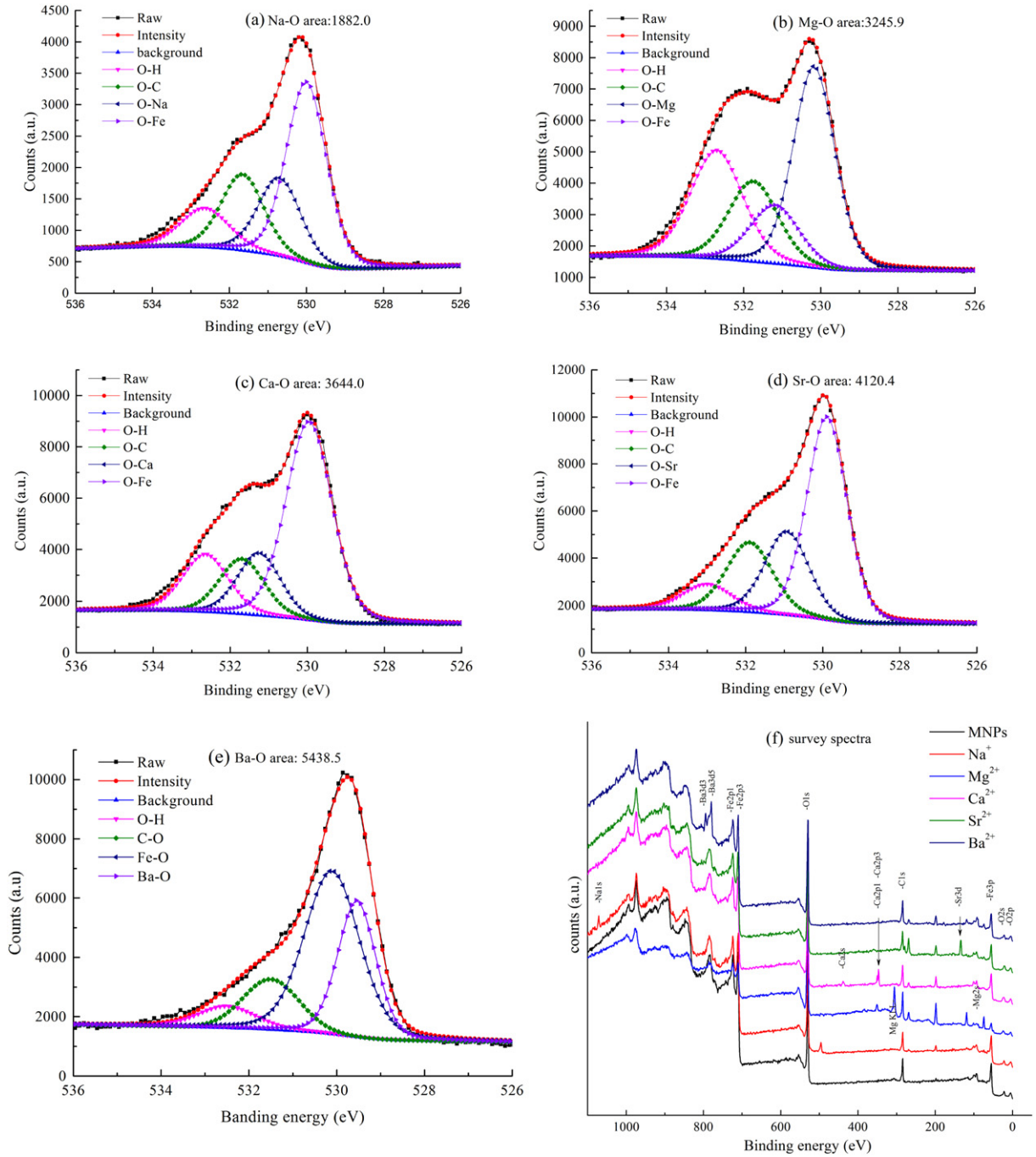

Fig. 6. XPS spectra of O 1s of Fe_3O_4 MNPs after the adsorption of metal cations at a pH of 9.0. (a) Na^+, (b) Mg^{2+}, (c) Ca^{2+}, (d) Sr^{2+}, (e) Ba^{2+}, and (f) survey spectra.

4. Conclusions

The aggregation of Fe_3O_4 MNPs was determined to be the result of the integrated effects of the pH of the matrix as well as concentration, valences, hydration forces and hydrated ionic radii of Na^+, Mg^{2+}, Ca^{2+}, Sr^{2+} and Ba^{2+} ions in aquatic environments. In addition to electrostatic force, magnetic attraction and the specific ion effect of metal cations should be significant parameters for predicting the aggregation of MNPs. Specifically, at a pH of 5.0, divalent cations potentially resulted in MNPs being resistant to aggregation due to a significantly increased NEB at their low concentrations. At a pH of 9.0, the different capacities of divalent cations for the aggregation of MNPs proved the significance of special ion effects, and the differences could be well-explained by the ionic radius, valence state and hydration energy of the metal cation.

Acknowledgements

This work was supported by the National Natural Science Foundation of China (No. 41222026, 41521003) and Science and Technology Basic Work (2014FY120600).

Appendix A. Supplementary data

Supplementary data to this article can be found online at http://dx.doi.org/10.1016/j.scitotenv.2017.02.060.

References

Aiken, G.R., Hsu-Kim, H., Ryan, J.N., 2011. Influence of dissolved organic matter on the environmental fate of metals, nanoparticles, and colloids. Environ. Sci. Technol. 45, 3196–3201.
Albanese, A., Chan, W.C.W., 2011. Effect of gold nanoparticle aggregation on cell uptake and toxicity. ACS Nano 5, 5478–5489.
Amal, R., Coury, J.R., Raper, J.A., Walsh, W.P., Waite, T.D., 1990. Structure and kinetics of aggregating colloidal haematite. Colloids Surf. 46, 1–19.
Ardizzone, S., Bianchi, C.L., Fadoni, M., Vercelli, B., 1997. Magnesium salts and oxide: an XPS overview. Appl. Surf. Sci. 119, 253–259.
Auffan, M., Rose, J., Bottero, J.-Y., Lowry, G.V., Jolivet, J.-P., Wiesner, M.R., 2009. Towards a definition of inorganic nanoparticles from an environmental, health and safety perspective. Nat. Nanotechnol. 4, 634–641.
Baalousha, M., 2009. Aggregation and disaggregation of iron oxide nanoparticles: influence of particle concentration, pH and natural organic matter. Sci. Total Environ. 407, 2093–2101.
Baalousha, M., Lead, J.R., 2012. Rationalizing nanomaterial sizes measured by atomic force microscopy, flow field-flow fractionation, and dynamic light scattering: sample preparation, polydispersity, and particle structure. Environ. Sci. Technol. 46, 6134–6142.
Badawy, A.M.E., Luxton, T.P., Silva, R.G., Scheckel, K.G., Suidan, M.T., Tolaymat, T.M., 2010. Impact of environmental conditions (pH, ionic strength, and electrolyte type) on the surface charge and aggregation of silver nanoparticles suspensions. Environ. Sci. Technol. 44, 1260–1266.
Bagchi, B., 2005. Water dynamics in the hydration layer around proteins and micelles. Chem. Rev. 105, 3197–3219.
Ben Ishai, P., Mamontov, E., Nickels, J.D., Sokolov, A.P., 2013. Influence of ions on water diffusion—a neutron scattering study. J. Phys. Chem. B 117, 7724–7728.
Berg, J.M., Romoser, A., Banerjee, N., Zebda, R., Sayes, C.M., 2009. The relationship between pH and zeta potential of ~ 30 nm metal oxide nanoparticle suspensions relevant to in vitro toxicological evaluations. Nanotoxicology 3, 276–283.
Bian, S.W., Mudunkotuwa, I.A., Rupasinghe, T., Grassian, V.H., 2011. Aggregation and dissolution of 4 nm ZnO nanoparticles in aqueous environments: influence of pH, ionic strength, size, and adsorption of humic acid. Langmuir 27, 6059–6068.
Bizmark, N., Ioannidis, M.A., 2015. Effects of ionic strength on the colloidal stability and interfacial assembly of hydrophobic ethyl cellulose nanoparticles. Langmuir 31, 9282–9289.
Borm, P.J.A., Robbins, D., Haubold, S., Kuhlbusch, T., Fissan, H., Donaldson, K., Schins, R., Stone, V., Kreyling, W., Lademann, J., 2006. The potential risks of nanomaterials: a review carried out for ECETOC. Part. Fibre Toxicol. 3, 11.
Boström, M., Williams, D.R.M., Ninham, B.W., 2001. Specific ion effects: why DLVO theory fails for biology and colloid systems. Phys. Rev. Lett. 87, 168103.
Bourikas, K., Hiemstra, T., Van Riemsdijk, W.H., 2001. Ion pair formation and primary charging behavior of titanium oxide (anatase and rutile). Langmuir 17, 749–756.
Boyd, C.E., Thunjai, T., 2003. Concentrations of major ions in waters of inland shrimp farms in China, Ecuador, Thailand, and the United States. J. World Aquacult. Soc. 34, 524–532.
Butler, R.F., Banerjee, S.K., 1975. Theoretical single-domain grain size range in magnetite and titanomagnetite. J. Geophys. Res. 80, 4049–4058.
Butter, K., Bomans, P.H.H., Frederik, P.M., Vroege, G.J., Philipse, A.P., 2003. Direct observation of dipolar chains in iron ferrofluids by cryogenic electron microscopy. Nat. Mater. 2, 88–91.
Chang, X., Bouchard, D.C., 2013. Multiwalled carbon nanotube deposition on model environmental surfaces. Environ. Sci. Technol. 47, 10372–10380.
Chaplin, M., 2008. Water Structure and Science. Aptarimas Vanduo. http://www1.lsbu.ac.uk/water/kosmotropes_chaotropes.html.
Chen, K.L., Elimelech, M., 2006. Aggregation and deposition kinetics of fullerene (C60) nanoparticles. Langmuir 22, 10994–11001.
Chen, K.L., Elimelech, M., 2007. Influence of humic acid on the aggregation kinetics of fullerene (C60) nanoparticles in monovalent and divalent electrolyte solutions. J. Colloid Interface Sci. 309, 126–134.
Chen, K.L., Mylon, S.E., Elimelech, M., 2006. Aggregation kinetics of alginate-coated hematite nanoparticles in monovalent and divalent electrolytes. Environ. Sci. Technol. 40, 1516–1523.
Chowdhury, I., Duch, M.C., Mansukhani, N.D., Hersam, M.C., Bouchard, D., 2013. Colloidal properties and stability of graphene oxide nanomaterials in the aquatic environment. Environ. Sci. Technol. 47, 6288–6296.
Christian, P., Von der Kammer, F., Baalousha, M., Hofmann, T., 2008. Nanoparticles: structure, properties, preparation and behaviour in environmental media. Ecotoxicology 17, 326–343.
Coppa, B.J., Davis, R.F., Nemanich, R.J., 2003. Gold Schottky contacts on oxygen plasma-treated, n-type ZnO(0001). Appl. Phys. Lett. 82, 400–402.
Crittenden, J.C., Trussell, R.R., Hand, D.W., Howe, K.J., Tchobanoglous, G., 2012. MWH's Water Treatment: Principles and Design. John Wiley & Sons, Inc., Hoboken.
de Vicente, J., Delgado, A.V., Plaza, R.C., Durán, J.D.G., González-Caballero, F., 2000. Stability of cobalt ferrite colloidal particles. Effect of pH and applied magnetic fields. Langmuir 16, 7954–7961.
Dumbre, D.K., Choudhary, V.R., Patil, N.S., Uphade, B.S., Bhargava, S.K., 2014. Calcium oxide supported gold nanoparticles as catalysts for the selective epoxidation of styrene by t-butyl hydroperoxide. J. Colloid Interface Sci. 415, 111–116.
Dumont, F., Warlus, J., Watillon, A., 1990. Influence of the point of zero charge of titanium dioxide hydrosols on the ionic adsorption sequences. J. Colloid Interface Sci. 138, 543–554.
Dzidic, I., Kebarle, P., 1970. Hydration of the alkali ions in the gas phase. Enthalpies and entropies of reactions M^+ (H2O) n-1$^+$ H2O═ M^+ (H2O) n. J. Phys. Chem. 74, 1466–1474.
Farré, M., Gajda Schrantz, K., Kantiani, L., Barceló, D., 2009. Ecotoxicity and analysis of nanomaterials in the aquatic environment. Anal. Bioanal. Chem. 393, 81–95.
Faure, B., Salazar-Alvarez, G., Bergström, L., 2011. Hamaker constants of iron oxide nanoparticles. Langmuir 27, 8659–8664.
Fiorino, D.J., 2010. Voluntary initiatives, regulation, and nanotechnology oversight: charting a path. Proj. Emerg. Nanotechnol. 19.
Förstner, U., Wittmann, G.T.W., 2012. Metal Pollution in the Aquatic Environment. Springer Science & Business Media.
Franks, G.V., 2002. Zeta potentials and yield stresses of silica suspensions in concentrated monovalent electrolytes: isoelectric point shift and additional attraction. J. Colloid Interface Sci. 249, 44–51.
French, R.A., Jacobson, A.R., Kim, B., Isley, S.L., Penn, R.L., Baveye, P.C., 2009. Influence of ionic strength, pH, and cation valence on aggregation kinetics of titanium dioxide nanoparticles. Environ. Sci. Technol. 43, 1354–1359.
Ghijsen, J., Namba, H., Thiry, P.A., Pireaux, J.J., Caudano, P., 1981. Adsorption of oxygen on the magnesium (0001) surface studied by XPS. Appl. Surf. Sci. 8, 397–411.
Godinez, I.G., Darnault, C.J.G., 2011. Aggregation and transport of nano-TiO2 in saturated porous media: effects of pH, surfactants and flow velocity. Water Res. 45, 839–851.
Grasso, D., Subramaniam, K., Butkus, M., Strevett, K., Bergendahl, J., 2002. A review of non-DLVO interactions in environmental colloidal systems. Rev. Environ. Sci. Biotechnol. 1, 17–38.
Guo, L., Hunt, B.J., Santschi, P.H., 2001. Ultrafiltration behavior of major ions (Na, Ca, Mg, F, Cl, and SO4) in natural waters. Water Res. 35, 1500–1508.
Hem, J.D., 1970. Study and Interpretation of the Chemical Characteristics of Natural Water. second ed. Department of the Interior, US Geological Survey, Washington, D.C.
House, J.E., House, K.A., 2015. Descriptive Inorganic Chemistry. second ed. Academic Press.
Illés, E., Tombácz, E., 2006. The effect of humic acid adsorption on pH-dependent surface charging and aggregation of magnetite nanoparticles. J. Colloid Interface Sci. 295, 115–123.
Jalali, M., Jalali, M., 2016. Geochemistry and background concentration of major ions in spring waters in a high-mountain area of the Hamedan (Iran). J. Geochem. Explor. 165, 49–61.
Johnson, R.L., Johnson, G.O.B., Nurmi, J.T., Tratnyek, P.G., 2009. Natural organic matter enhanced mobility of nano zerovalent iron. Environ. Sci. Technol. 43, 5455–5460.
Klaine, S.J., Alvarez, P.J., Batley, G.E., Fernandes, T.F., Handy, R.D., Lyon, D.Y., Mahendra, S., McLaughlin, M.J., Lead, J.R., 2008. Nanomaterials in the environment: behavior, fate, bioavailability, and effects. Environ. Toxicol. Chem. 27, 1825–1851.
Kunz, W., 2010. Specific ion effects in colloidal and biological systems. Curr. Opin. Colloid Interface Sci. 15, 34–39.
Li, W., Liu, D., Wu, J., Kim, C., Fortner, J.D., 2014. Aqueous aggregation and surface deposition processes of engineered superparamagnetic iron oxide nanoparticles for environmental applications. Environ. Sci. Technol. 48, 11892–11900.
Lin, D., Tian, X., Wu, F., Xing, B., 2010. Fate and transport of engineered nanomaterials in the environment. J. Environ. Qual. 39, 1896–1908.
Lo Nostro, P., Ninham, B.W., 2012. Hofmeister phenomena: an update on ion specificity in biology. Chem. Rev. 112, 2286–2322.
López León, T., Jódar Reyes, A.B., Bastos González, D., Ortega Vinuesa, J.L., 2003. Hofmeister effects in the stability and electrophoretic mobility of polystyrene latex particles. J. Phys. Chem. B 107, 5696–5708.

López León, T., Jódar Reyes, A.B., Ortega Vinuesa, J.L., Bastos González, D., 2005. Hofmeister effects on the colloidal stability of an IgG-coated polystyrene latex. J. Colloid Interface Sci. 284, 139–148.
Lu, A., Salabas, E.L., Schüth, F., 2007. Magnetic nanoparticles: synthesis, protection, functionalization, and application. Angew. Chem. Int. Ed. 46, 1222–1244.
McGrail, B.P., Icenhower, J.P., Shuh, D.K., Liu, P., Darab, J.G., Baer, D.R., Thevuthasen, S., Shutthanandan, V., Engelhard, M.H., Booth, C.H., Nachimuthu, P., 2001. The structure of Na2O–Al2O3–SiO2 glass: impact on sodium ion exchange in H2O and D2O. J. Non-Cryst. Solids 296, 10–26.
Moore, M.N., 2006. Do nanoparticles present ecotoxicological risks for the health of the aquatic environment? Environ. Int. 32, 967–976.
O'Brien, N.J., Cummins, E.J., 2011. A risk assessment framework for assessing metallic nanomaterials of environmental concern: aquatic exposure and behavior. Risk Anal. 31, 706–726.
Oncsik, T., Trefalt, G., Borkovec, M., Szilagyi, I., 2015. Specific ion effects on particle aggregation induced by monovalent salts within the Hofmeister series. Langmuir 31, 3799–3807.
Pankhurst, Q.A., Connolly, J., Jones, S.K., Dobson, J., 2003. Applications of magnetic nanoparticles in biomedicine. J. Phys. D. Appl. Phys. 36, R167.
Parsons, D.F., Bostrom, M., Nostro, P.L., Ninham, B.W., 2011. Hofmeister effects: interplay of hydration, nonelectrostatic potentials, and ion size. PCCP 13, 12352–12367.
Pashley, R.M., 1981. DLVO and hydration forces between mica surfaces in Li^+, Na^+, K^+, and Cs^+ electrolyte solutions: a correlation of double-layer and hydration forces with surface cation exchange properties. J. Colloid Interface Sci. 83, 531–546.
Pashley, R.M., Israelachvili, J.N., 1984. Dlvo and hydration forces between mica surfaces in Mg^{2+}, Ca^{2+}, Sr^{2+}, and Ba^{2+} chloride solutions. J. Colloid Interface Sci. 97, 446–455.
Pham, M., Mintz, E.A., Nguyen, T.H., 2009. Deposition kinetics of bacteriophage MS2 to natural organic matter: role of divalent cations. J. Colloid Interface Sci. 338, 1–9.
Phenrat, T., Saleh, N., Sirk, K., Tilton, R.D., Lowry, G.V., 2007. Aggregation and sedimentation of aqueous nanoscale zerovalent iron dispersions. Environ. Sci. Technol. 41, 284–290.
Philippe, A., Schaumann, G.E., 2014. Interactions of dissolved organic matter with natural and engineered inorganic colloids: a review. Environ. Sci. Technol. 48, 8946–8962.
Rance, G.A., Marsh, D.H., Bourne, S.J., Reade, T.J., Khlobystov, A.N., 2010. van der Waals interactions between nanotubes and nanoparticles for controlled assembly of composite nanostructures. ACS Nano 4, 4920–4928.
Reddy, L.H., Arias, J.L., Nicolas, J., Couvreur, P., 2012. Magnetic nanoparticles: design and characterization, toxicity and biocompatibility, pharmaceutical and biomedical applications. Chem. Rev. 112, 5818–5878.
Rodgers, M.T., Armentrout, P.B., 2016. Cationic noncovalent interactions: energetics and periodic trends. Chem. Rev.
Rodriguez-Cruz, S.E., Jockusch, R.A., Williams, E.R., 1999. Hydration energies and structures of alkaline earth metal ions, M^{2+} (H2O) n, n = 5–7, M = Mg, Ca, Sr, and Ba. J. Am. Chem. Soc. 121, 8898–8906.
Saleh, N.B., Pfefferle, L.D., Elimelech, M., 2008. Aggregation kinetics of multiwalled carbon nanotubes in aquatic systems: measurements and environmental implications. Environ. Sci. Technol. 42, 7963–7969.
Saleh, N.B., Pfefferle, L.D., Elimelech, M., 2010. Influence of biomacromolecules and humic acid on the aggregation kinetics of single-walled carbon nanotubes. Environ. Sci. Technol. 44, 2412–2418.
Sano, M., Okamura, J., Shinkai, S., 2001. Colloidal nature of single-walled carbon nanotubes in electrolyte solution: the Schulze–Hardy rule. Langmuir 17, 7172–7173.
Scholten, P.C., 1983. How magnetic can a magnetic fluid be? J. Magn. Magn. Mater. 39, 99–106.
Seiichi, K., Tatsuo, I., Ikuo, A., 2006. Adsorption Science. chemical industry press, Beijing, pp. 31–34.
Sharma, V.K., 2009. Aggregation and toxicity of titanium dioxide nanoparticles in aquatic environment—a review. J. Environ. Sci. Health A 44, 1485–1495.
Sun, Y., Wang, X., Ding, C., Cheng, W., Chen, C., Hayat, T., Alsaedi, A., Hu, J., Wang, X., 2016. Direct synthesis of bacteria-derived carbonaceous nanofibers as a highly efficient material for radionuclides elimination. ACS Sustain. Chem. Eng. 4, 4608–4616.
Vance, M.E., Kuiken, T., Vejerano, E.P., McGinnis, S.P., Hochella Jr., M.F., Rejeski, D., Hull, M.S., 2015. Nanotechnology in the real world: redeveloping the nanomaterial consumer products inventory. Beilstein J. Nanotechnol. 6, 1769–1780.
Vasquez, R.P., 1991. X-ray photoelectron spectroscopy study of Sr and Ba compounds. J. Electron Spectrosc. Relat. Phenom. 56, 217–240.
Verrall, K.E., Warwick, P., Fairhurst, A.J., 1999. Application of the Schulze–Hardy rule to haematite and haematite/humate colloid stability. Colloids Surf. A 150, 261–273.
Wang, H., Zhao, X., Meng, W., Wang, P., Wu, F., Tang, Z., Han, X., Giesy, J.P., 2015. Cetyltrimethylammonium bromide-coated Fe3O4 magnetic nanoparticles for analysis of 15 trace polycyclic aromatic hydrocarbons in aquatic environments by ultraperformance, liquid chromatography with fluorescence detection. Anal. Chem. 87, 7667–7675.
Wiesner, M.R., Lowry, G.V., Alvarez, P., Dionysiou, D., Biswas, P., 2006. Assessing the risks of manufactured nanomaterials. Environ. Sci. Technol. 40, 4336–4345.
Wu, F., Xing, B., 2009. Natural Organic Matter and Its Significance in the Environment. Science Press, Beijing.
Yamashita, T., Hayes, P., 2008. Analysis of XPS spectra of Fe^{2+} and Fe^{3+} ions in oxide materials. Appl. Surf. Sci. 254, 2441–2449.
Yu, S., Wang, X., Ai, Y., Liang, Y., Ji, Y., Li, J., Hayat, T., Alsaedi, A., Wang, X., 2016. Spectroscopic and theoretical studies on the counterion effect of Cu(ii) ion and graphene oxide interaction with titanium dioxide. Environ. Sci.: Nano 3, 1361–1368.
Zhang, W., Elliott, D.W., 2006. Applications of iron nanoparticles for groundwater remediation. Remediat. J. 16, 7–21.
Zhang, Y., Chen, Y., Westerhoff, P., Crittenden, J., 2009. Impact of natural organic matter and divalent cations on the stability of aqueous nanoparticles. Water Res. 43, 4249–4257.
Zhao, X., Shi, Y., Cai, Y., Mou, S., 2008a. Cetyltrimethylammonium bromide-coated magnetic nanoparticles for the preconcentration of phenolic compounds from environmental water samples. Environ. Sci. Technol. 42, 1201–1206.
Zhao, X., Shi, Y., Wang, T., Cai, Y., Jiang, G., 2008b. Preparation of silica-magnetite nanoparticle mixed hemimicelle sorbents for extraction of several typical phenolic compounds from environmental water samples. J. Chromatogr. A 1188, 140–147.
Zou, Y., Wang, X., Ai, Y., Liu, Y., Li, J., Ji, Y., Wang, X., 2016a. Coagulation behavior of graphene oxide on nanocrystallined Mg/Al layered double hydroxides: batch experimental and theoretical calculation study. Environ. Sci. Technol. 50, 3658–3667.
Zou, Y., Wang, X., Chen, Z., Yao, W., Ai, Y., Liu, Y., Hayat, T., Alsaedi, A., Alharbi, N.S., Wang, X., 2016b. Superior coagulation of graphene oxides on nanoscale layered double hydroxides and layered double oxides. Environ. Pollut. 219, 107–117.

Supporting Information

Effects of monovalent and divalent metal cations on the aggregation and suspension of Fe_3O_4 magnetic nanoparticles in aqueous solution

Hao Wang[a,b], Xiaoli Zhao[b,*], Xuejiao Han[b], Zhi Tang[b], Shasha Liu[a,b], Wenjing Guo[a,b], Huanhua Wang[b], Chaobing Deng[c], Qingwei Guo[d], Fengchang Wu[b], Xiaoguang Meng[b,e] John P. Giesy[b,f]

[a] *College of Water Sciences, Beijing Normal University, Beijing 100875, China.*

[b] *State Key Laboratory of Environmental Criteria and Risk Assessment, Chinese Research Academy of Environmental Sciences, Beijing 100012, China.*

[c] *Environmental Monitoring Center of Guangxi Zhuang Autonomous Region, Guangxi 530028, China.*

[d] *South China Institute of Environmental Science. MEP, Guangzhou 510655, China.*

[e] *Center for Environmental Systems, Stevens Institute of Technology, Hoboken, New Jersey 07030, United States.*

[f] *Department of Biomedical and Veterinary Biosciences and Toxicology Centre, University of Saskatchewan, Saskatoon, Saskatchewan, Canada.*

*Corresponding Author: zhaoxiaoli_zxl@126.com.

Tel.: (+86)10-84931804; Fax: (+86)10-84931804.

This supporting information contains 3 figures. This document contains 8 pages including this cover page.

2.1. Synthesis of Fe_3O_4 MNPs

The Fe_3O_4 MNPs used in this study were synthesized by co-precipitation (Zhao et al., 2008). Briefly, a 25 mL solution containing a mixture of 5.2 g of $FeCl_3 \cdot 6H_2O$, 2.0 g of $FeCl_2 \cdot 4H_2O$, 0.85 mL of HCl and dissolved oxygen-free water was added dropwise into 250 mL of NaOH solution at 75 °C under nitrogen gas with mechanical stirring at a speed of 430 r/min. Then, the solution containing generated Fe_3O_4 MNPs was washed with 200 mL of dissolved oxygen-free water several times to remove inorganic ions, and a DX223-Na sodium electrode (Mettler Toledo, Switzerland) was used to ensure that the concentration of Na^+ was less than 0.5 mM. Afterwards, the solution was diluted with ultrapure water to 110 mL to obtain a concentration of approximately 20 $mg \cdot mL^{-1}$ Fe_3O_4 MNPs.

2.2. Theoretical analysis of the aggregation of MNPs

DLVO theory is extensively used to analyze the aggregation of particles in aqueous solutions and suspensions by quantifying the interactions in the micro-interface of colloids (Elimelech et al., 2013; Hu et al., 2010; Zhang et al., 2009; Zhang et al., 2008). However, when given the significant effects of non-electrostatic ionic forces such as ionic dispersion force and induction force on a colloidal system at a high salt concentration (e.g., more than 100.0 mM), the traditional DLVO theory failed to predict the behavior of colloids, especially for biological systems (Boström et al., 2001; Grasso et al., 2002; López León et al., 2005; Lo Nostro and Ninham, 2012). In natural bulk aquatic environments, the concentrations of major ions are generally below 100.0 mM; thus, traditional DLVO theory could work well for a

natural bulk aquatic environment (Boström et al., 2001; López León et al., 2005). However, due to the effect of the inherent permanent magnetic dipole moment of MNPs, the suspension of MNPs should also be affected by magnetic attraction in addition to van der Waals (V_{vdW}) and electrostatic energies (V_{ES}). When the dipoles of MNPs are presented in a head-to-tail configuration, the maximum magnetic energy (V_M) between them is described by equation (S4) (Phenrat et al., 2007).

$$V_{Total} = V_{vdW} + V_{EDL} + V_M \quad \text{(S1)}$$

$$V_{vdW} = \frac{-A}{6}\left[\frac{2r^2}{H(H+4r)} + \frac{2r^2}{(H+2r)^2} + \ln\frac{H(H+4r)}{(H+2r)^2}\right] \quad \text{(S2)}$$

$$V_{EDL} = \frac{4\pi\varepsilon r^2\zeta^2}{H+2r} exp^{(-\kappa \cdot H)} \quad \text{(S3)}$$

$$V_M = \frac{-8\pi\mu_0 M_s^2 r^3}{9\left(\frac{H}{r}+2\right)^3} \quad \text{(S4)}$$

where A is the Hamaker constant (J); r is the particle radius (m); ε is the dielectric constant of water at 298 K; ζ is the surface potential of a particle; κ is the reciprocal of the radius of an ionic atmosphere (Debye length); μ_0 is the permeability of the vacuum ($H \cdot m^{-1}$); and M_s is the saturation magnetization ($3.13\times10^5 A \cdot m^{-1}$) (Zhao, 2009; Zhao et al., 2008).

2.3 Calculation of the adsorption ratio of cations on MNPs

In the study, the adsorption ratio (r) was calculated from the absolute adsorption amount (A) divided by the total amount (T). The equation is as follows:

$$r = \frac{A}{T}$$

3. Results

3.1. Characteristics of Fe_3O_4 MNPs

The Fe_3O_4 MNPs synthesized in the study had a diameter of approximately10 nm

and were highly crystallized (Fig. S1a and b). The as-synthesized MNPs were face centered cubic particles according to the XRD pattern (Hu et al., 2010). They were further characterized by use of the Nano-Measurer 1.2.5 software, and they have a mean diameter of 11.7 nm with a range of 5~25 nm (Fig. S1c). The size of these as-prepared MNPs was below 80 nm, the critical size of the multiple magnetic domain for MNPs. Thus, the MNPs of the study are assumed to be single magnetic domain particles and presented excellent magnetic properties (Butler and Banerjee, 1975; Phenrat et al., 2007). Therefore, the MNPs exhibited a tendency foraggregation, which has been previously observed, previously due to theirits inherent permanent magnetic dipole moment (Butter et al., 2003; Liu et al., 2005; Phenrat et al., 2007).

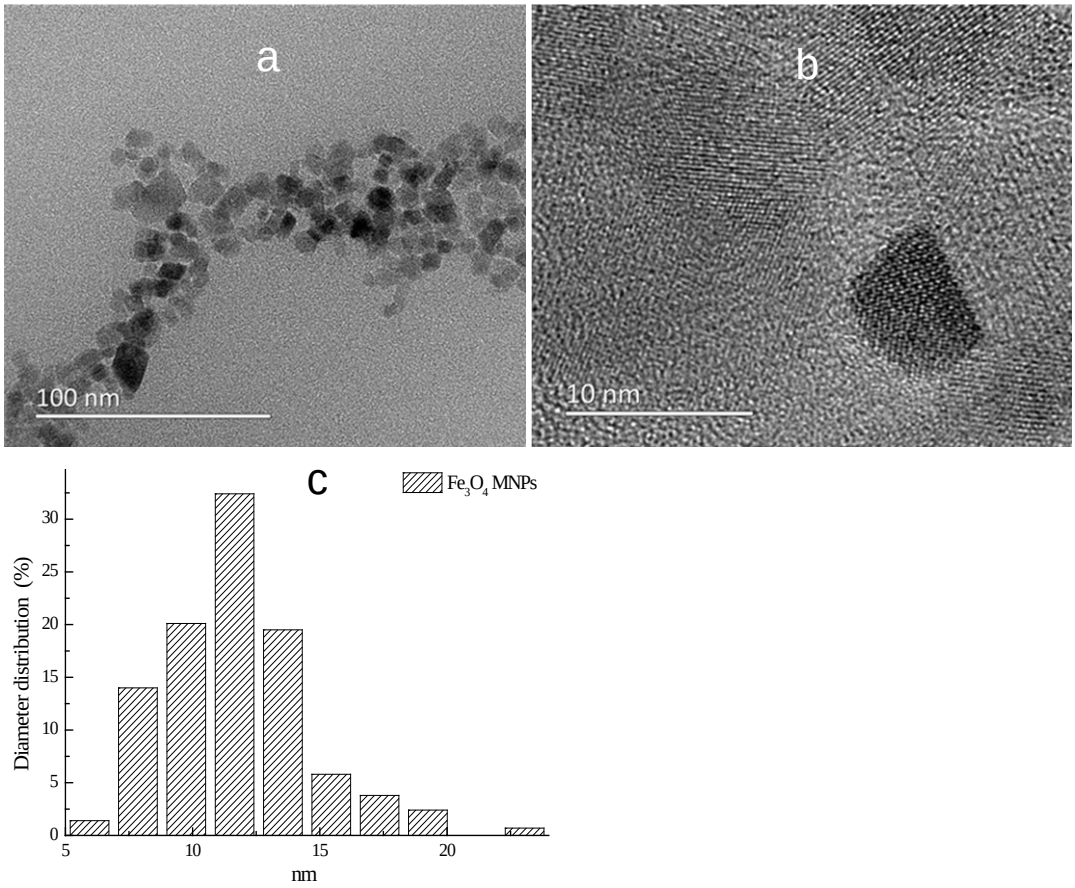

Fig. S1. TEM images (a, b) and size distribution (c) of Fe_3O_4 MNPs .

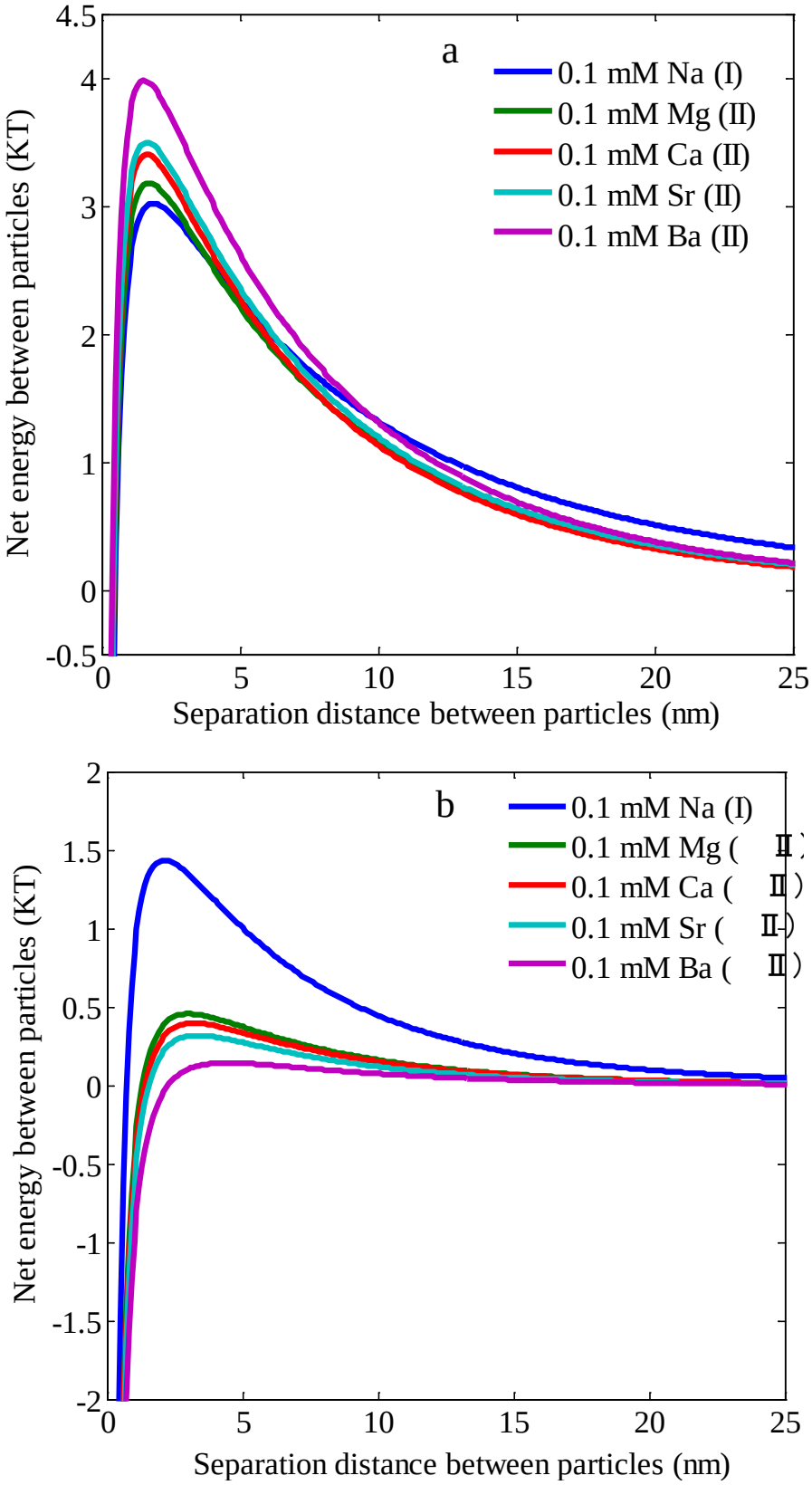

Fig. S2. Net energies between particles by extended DLVO theory under the effect of a 0.1 mM solution of the five metal cations at pH values of 5.0 (a) and 9.0 (b).

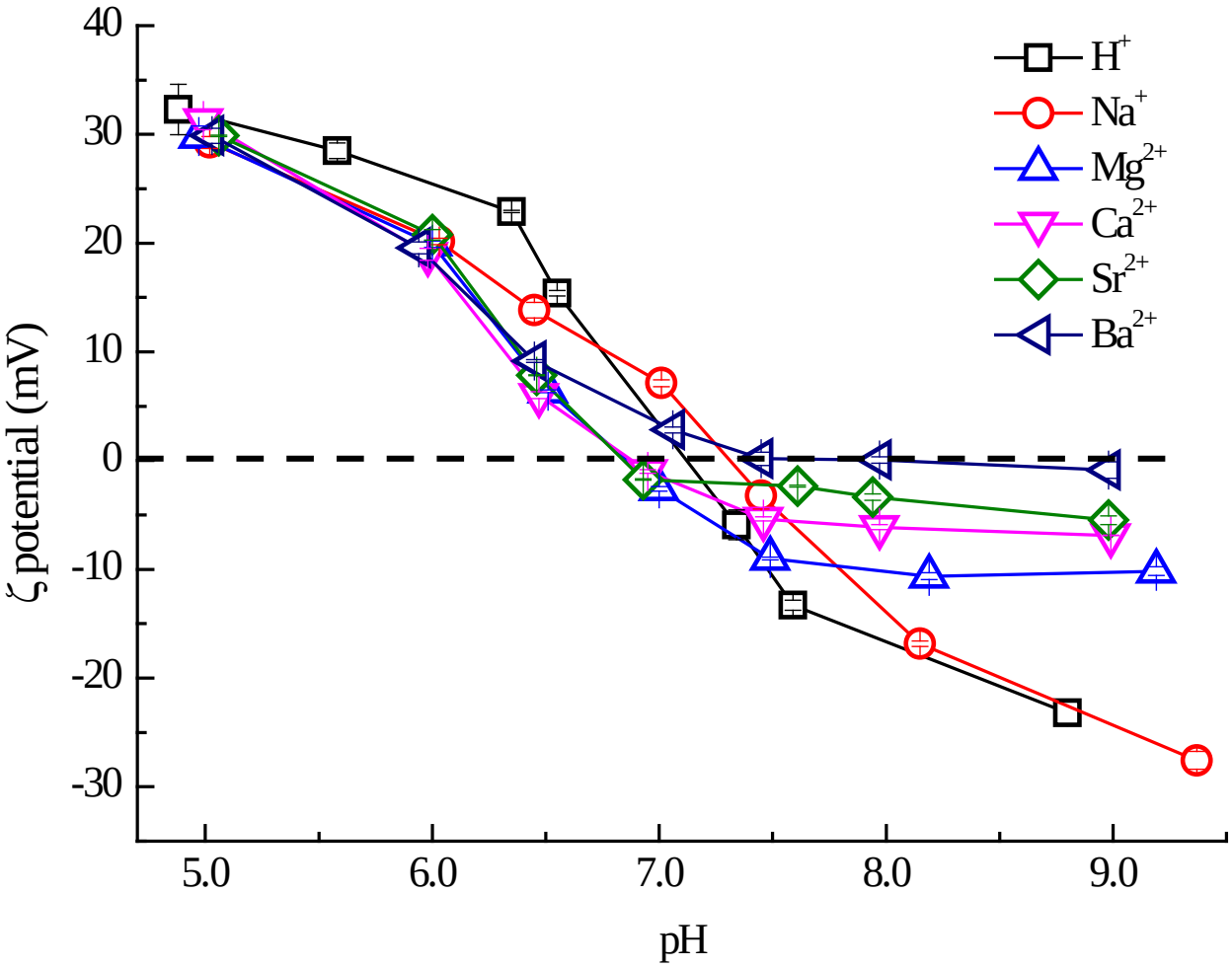

Fig. S3. Effect of the pH on the ζ potential of Fe_3O_4 MNPs under a 0.1 mM solution of the five metal cations.

References

Boström, M., Williams, D.R.M., Ninham, B.W., 2001. Specific Ion Effects: Why DLVO Theory Fails for Biology and Colloid Systems. Phys. Rev. Lett. 87, 168103.

Butler, R.F., Banerjee, S.K., 1975. Theoretical single-domain grain size range in magnetite and titanomagnetite. J. Geophys. Res. 80, 4049-4058.

Butter, K., Bomans, P.H.H., Frederik, P.M., Vroege, G.J., Philipse, A.P., 2003. Direct observation of dipolar chains in iron ferrofluids by cryogenic electron microscopy. Nat. Mater. 2, 88-91.

Elimelech, M., Gregory, J., Jia, X., 2013. Particle deposition and aggregation: measurement, modelling and simulation. Butterworth-Heinemann.

Grasso, D., Subramaniam, K., Butkus, M., Strevett, K., Bergendahl, J., 2002. A review of non-DLVO interactions in environmental colloidal systems. Rev. Environ. Sci. Biotechnol. 1, 17-38.

Hu, J., Zevi, Y., Kou, X., Xiao, J., Wang, X., Jin, Y., 2010. Effect of dissolved organic matter on the stability of magnetite nanoparticles under different pH and ionic strength conditions. Sci. Total Environ. 408, 3477-3489.

López León, T., Jódar Reyes, A.B., Ortega Vinuesa, J.L., Bastos González, D., 2005. Hofmeister effects on the colloidal stability of an IgG-coated polystyrene latex. J. Colloid Interface Sci. 284, 139-148.

Liu, Y., Majetich, S.A., Tilton, R.D., Sholl, D.S., Lowry, G.V., 2005. TCE Dechlorination Rates, Pathways, and Efficiency of Nanoscale Iron Particles with Different Properties. Environ. Sci. Technol. 39, 1338-1345.

Lo Nostro, P., Ninham, B.W., 2012. Hofmeister Phenomena: An Update on Ion Specificity in Biology. Chem. Rev. 112, 2286-2322.

Phenrat, T., Saleh, N., Sirk, K., Tilton, R.D., Lowry, G.V., 2007. Aggregation and Sedimentation of Aqueous Nanoscale Zerovalent Iron Dispersions. Environ. Sci. Technol. 41, 284-290.

Zhang, Y., Chen, Y., Westerhoff, P., Crittenden, J., 2009. Impact of natural organic matter and divalent cations on the stability of aqueous nanoparticles. Water Res. 43, 4249-4257.

Zhang, Y., Chen, Y., Westerhoff, P., Hristovski, K., Crittenden, J.C., 2008. Stability of commercial metal oxide nanoparticles in water. Water Res. 42, 2204-2212.

Zhao, X., 2009. Application potentials of novel magnetic nanoparticles as sorbent materials in environmental science and analytical chemistry, Research center for Eco-environmental science. Chinese academy of sciences, Beijing.

Zhao, X., Shi, Y., Cai, Y., Mou, S., 2008. Cetyltrimethylammonium Bromide-Coated Magnetic Nanoparticles for the Preconcentration of Phenolic Compounds from Environmental Water Samples. Environ. Sci. Technol. 42, 1201-1206.